Level-1 Calibration Assessment of Spire's LEMUR-2 GNSS-R Ocean Normalized Bistatic Radar Cross Section Estimates

Mohammad M. Al-Khaldi, *Member, IEEE,* Scott Gleason, *Senior Member, IEEE,*
Ryan Linnabary and Frederick S. Policelli

***Abstract*—An assessment of the ocean surface Level-1 Normalized Bistatic Radar Cross Section products provided by the two batch 1 'LEMUR-2' GNSS-R receivers of Spire, Inc. is reported. The analysis uses datasets extending from DOY 345, 2020 to DOY 329, 2021. Initial assessments indicate a highly consistent overall inter-channel response with mean NBRCS differences estimated to be at the 1.00% level over a 7-12 m/s ECMWF reference wind speed range. Efforts to validate the observation systems' aggregate response relative to ≈3 million co-located CYGNSS measurements suggest a highly complementary behavior with an overall NBRCS correlation of 79.03% highlighting the potential utility of 'LEMUR-2' measurements for ocean surface wind sensing and related applications. Non-physical NBRCS dependencies on various Level-1 calibration variables, also observed with GNSS-R previous systems, are nonetheless noted and are explored in detail.**

***Index Terms*—Global Navigation Satellite Systems Reflectometry (GNSS-R), CubeSats, SmallSats, bistatic radar systems, rough surface scattering**

I. Introduction

THE emergence of Global Navigation Satellite System Reflectometry sensors provides an opportunity to meet the concurrent needs for low cost, short incubation time, moderate spatial resolution and low latency in microwave remote sensing of Earth's surface. These factors have provided impetus for commercial vendors such as Spire, Inc. to launch multiple GNSS-R observatories with the goal of producing multiple sustained and commercially viable Earth surface geophysical products.

The utility of any derived Level-2 science products is directly related to the impact of calibration uncertainties in the associated Level-1 data. This is especially important in the case of GNSS-R receivers given the fact that each receiver is typically capable of tracking multiple reflections simultaneously such that measurements formed over a given integration period may be susceptible to Flight Module (FM) or channel specific biases potentially compromising the quality of the calibration applied to Level-1 DDMs. This is further compounded by the fact that specularly reflected transmissions originate from GNSS (Global Navigation Satellite System) space vehicles whose properties are not fully characterized and can change over time.

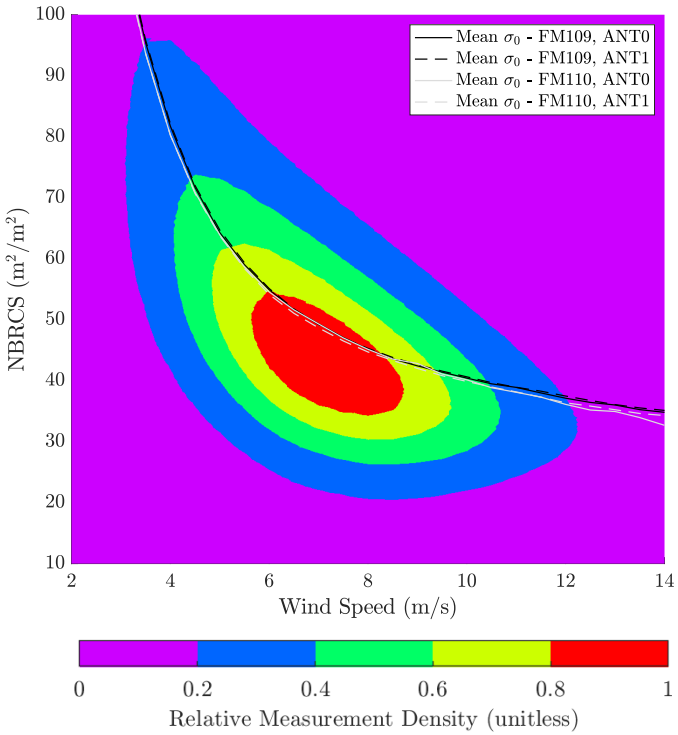

Fig. 1: Density plot summarizing Spire observatories' NBRCS correspondence to reference ECMWF surface winds interpolated to FM109 and FM110 time of observation and location within 0.5 NBRCS bins and 0.5 m/s wind speed bins.

Given the importance of accurate Level-1 calibration, this work overviews assessments of Spire GNSS-R receivers' 'L1b' NBRCS estimates over the ocean as part of an ongoing partnership with NASA's Commercial Smallsat Data Acquisition (CSDA) Program. While Spire's receivers also provide observables over land, the more complex nature of land returns as compared to ocean reflections [1]–[3] motivates that the corresponding land surface assessments be reported separately.

II. Instrument Description

The analysis focuses on Spire's two Batch-1 'LEMUR-2' GNSS-R receivers, FM109 and FM110, both launched in

The research of this article is supported by the NASA CSDA Program Grant Number 80NSSC21K0773.

M. M. Al-Khaldi is with the Department of Electrical and Computer Engineering and ElectroScience Laboratory, The Ohio State University, Columbus, OH 43210 USA.

S. Gleason is with DAAXA LLC, Boulder, CO 80305 USA

F. S. Policelli is with the Hydrological Sciences Laboratory, NASA Goddard Space Flight Center, Greenbelt, MD 20771 USA.

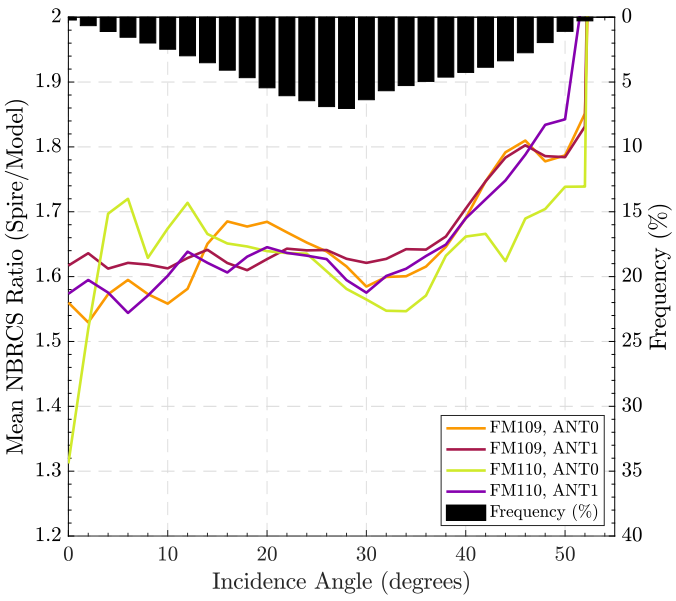

Fig. 2: Mean Spire/Model NBRCS Ratio vs incidence angle binned by FM (109, 110) and science antenna (ANT0, ANT1) over 7-12 m/s wind speeds

December of 2019 and placed in Low Earth Orbit (LEO). Both FMs 109 and 110 have a 3U (10×10×30 cm) form factor, a 3-axis attitude control system, a ground communication system using UHF and S-band elements, and an RF front end, digital processor, and calibration board. The zenith RHCP (right hand circularly polarized) antenna has a 5 dB peak gain, and the two nadir LHCP (left hand circularly polarized) antennas used for science measurements have 9.6 dB peak antenna gain [4]. The batch 1 satellites offer a number of unique capabilities compared to existing GNSS-R receivers including the ability to process reflections from a wide range of GNSS constellations (such as QZSS, Galileo and BDS) beyond the GPS constellation. For the dataset used in this work, specular measurements corresponded 59.42%, 3.80%, 25.41% and 11.37% to the GPS, QZSS, Galileo and BDS constellations, respectively. Given the orbital ≈37° inclination of the instruments, the limits of latitude coverage are approximately ±40°.

Spire's GNSS-R products over both land and ocean surfaces begin as uncalibrated 'raw' Level-0 DDMs that are later calibrated to Level 1a bistatic radar cross section (BRCS) DDMs as an initial step prior to separating all ocean observations to an independent Level 1b-Ocean dataset containing NBRCS estimates. The GNSS-R Level-1 calibration process used to estimate NBRCS follows similar architectures previously outlined in [5], [6] that are not reviewed in further detail here.

To highlight the utility of Spire σ_0 estimates for ocean surface wind estimation, Fig. 1 depicts a 2-D relative density plot using all available σ_0 estimates provided by the two Spire FMs relative to spatially and temporally interpolated reference ECMWF (European Centre for Medium-Range Weather Forecasts) surface wind estimates u_{10}. The general monotonic decline in NBRCS with wind speed follows expected behaviors given the related increase in surface roughness. Over the 5-12 m/s wind speed range, the mean sensitivity $\overline{S}$ is 2.30 (m^2/m^2)/(m/s). Initial assessments also indicate a highly consistent overall inter-channel response, with mean NBRCS differences estimated to be at the 1.00% level over a 5-12 m/s ECMWF reference wind speed range.

III. Observation Geometry Dependencies

Specular GNSS-R measurements occur at a variety of incidence and azimuth angles, and modest inaccuracies in antenna pattern predictions may lead to channel-specific NBRCS biases. A key validation criteria relates to investigating NBRCS dependencies on specular point incidence angles. This is complicated by the natural variability of surface roughness as a function of incidence angle [7]. To account for this variability, Spire's NBRCS estimates are normalized by model NBRCS estimates generated using the geometrical optics (GO) approximation and an ocean surface spectrum described by the Elfouhaily et al. model [8] similar to that proposed in [9]. The resulting ratios are summarized in Fig. 2, which reports mean NBRCS ratio estimates provided by the two science antennas of FM109 and FM110 across different wind speed regimes. In this context, a perfectly calibrated antenna pattern should be associated with an NBRCS ratio of 1. An NBRCS ratio exceeding 1 indicates an underestimation of on-board antenna pattern gain levels, while a ratio lower than 1 indicates an overestimation of gain. It is noted that the interpretation of the results in terms of ratio magnitudes is inherently limited by the representativeness of the model NBRCS estimates and related ancillary ocean surface information at the time of the receivers' observations, for a more comprehensive overview see [9]. For this reason, the interest in this section is not in the magnitude of the NBRCS ratios but rather their variability as a function of incidence angle. Such variations are expected to be more representative of considerations related to Level-1 calibration, namely any progressively increasing errors associated with the estimation of the receive antenna pattern gain levels as a function of incidence angle.

The results depicted in Fig. 2 suggest that NBRCS ratios are positively correlated with incidence angle such that the related estimates undergo a near monotonic increase of up to 96% relative to the mean over an incidence angle range 0-50°. Because the related error statistics can vary appreciably within different incidence angle ranges, statistics were also computed with the dataset further separated into incidence angle ranges described as 'low' ($\theta_i \leq 10°$, the angles lower than the 10th percentile point in the measurements' incidence angle CDF), 'high' ($\theta_i \geq 42°$, the angles exceeding the 90th percentile point in the measurements' incidence angle CDF) and 'overall' ($8° \leq \theta_i \leq 48°$, the angles over which 90% of the data exists relative to the incidence angle PDF mode). Using measurements falling within the 'overall' wind speed and incidence angle ranges, the average root mean square difference (RMSD) is estimated to be on the order of 3.91% as evidenced by the 'flatness' of the NBRCS vs incidence angle curves over the relevant angles in Fig. 2. The mean RMSD increases however to an average of 49.53% for the 'high' incidence angles, as evidenced by the steep slopes starting at $\approx \theta_i \geq 38°$, with a maximum RMSD of 78.51% occurring for

TABLE I: Spire/Model NBRCS ratio dependence on incidence angle within the medium wind speed regime, 7-12 m/s

θ_i **Range**	**NBRCS Ratio Mean** (m^2/m^2)	**NBRCS Ratio RMSD** (%)	**NBRCS Ratio Slope**
Overall ($8 \leq \theta_i \leq 48°$)	1.65	3.71	0.00
Low ($\theta_i \leq 10°$)	1.59	2.94	0.01
High ($\theta_i \geq 42°$)	6.26	53.12	0.20

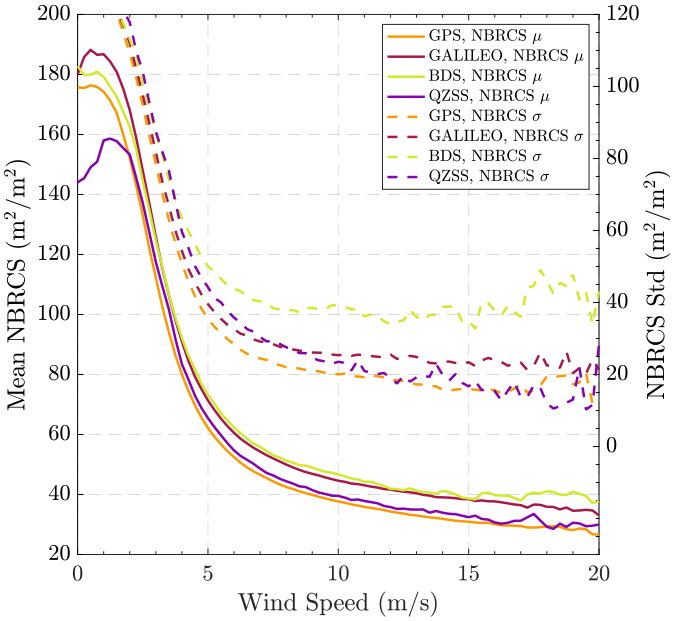

Fig. 3: Overall Spire LEMUR-2 receivers' NBRCS mean μ and standard deviation σ as a function of reference wind speed (Δu_{10} = 0.25 m/s) binned by transmitting GNSS constellation.

FM109, ANT0. Additionally, the increased RMSD at higher incidence angles is also expected to be attributable, in part, to reduced receive antenna gain levels.

IV. Transmitter Dependencies

A factor significantly complicating the calibration of GNSS-R measurements is their reliance on reflections from independent GNSS transmissions whose transmit power levels are not precisely known. Reference [10] has highlighted inter-transmitter biases in L1 calibrated σ_0 estimates of up to $\approx$2 dB (or equivalently 1.58 m^2/m^2) that can result from these effects. This necessitates in-orbit real time tracking of transmit EIRP levels for each measurement as first demonstrated by CYGNSS's eight satellite constellation [11].

Fig. 3 depicts mean NBRCS estimates from FM109 and FM110 versus reference ECMWF wind speeds in which the reflections arising from different GNSS transmissions including GPS, Galileo, BDS and QZSS are separated. The results confirm a bifurcation of the NBRCS into two distinct groups. Results for the GPS and QZSS transmissions have highly comparable means of 36.73 and 38.55 m^2/m^2 respectively across a wind speed range of 5-20 m/s. Reflections from Galileo and BDS transmissions in contrast have means of 44.06 and 46.13 m^2/m^2, respectively, suggesting an average difference ranging between 6-10 m^2/m^2 across the two families of transmitters. The NBRCS standard deviation in each wind speed bin is also depicted in Fig. 3, and shows that the GPS, Galileo and QZSS constellations have similar standard deviations on the order of 22.39 m^2/m^2 from 5-20 m/s while BDS standard deviations are markedly higher (an average of 39.54 m^2/m^2 over the same wind speed range). The BDS difference in standard deviation is 18.08 m^2/m^2 relative to GPS (associated with the lowest average uncertainty) at 10.75 m/s and 29.45 m^2/m^2 at 17.25 m/s.

Differences in the characteristics of transmitted signals across different GNSS transmitter families are associated with their system requirements for propagation link budgets, minimum received signal power levels, transmit and receive antenna gains, and estimated polarization or atmospheric loss effects. Real time transmit power levels have further been shown to depart from their nominal values by 2-4 dBs (or equivalently 1.58-2.51 m^2/m^2) [11]. Independent assessments of the actual transmitted powers [12] suggest average power levels on the order of 244, 193, 165, and 158 Watts for the QZSS, GPS (excluding block IIA and IIR-A/B transmitters the bulk of which have been retired or declared unhealthy), Galileo and BDS transmitters respectively. While it is noted that these are average estimates with individual transmitters potentially broadcasting signal intensities at slightly above or below mean levels, the average constellation specific transmit power levels suggest that the existing calibration scheme may be associated with some level of dependence on transmit power levels given that the two GNSS systems with the highest power levels, QZSS and GPS, form the first common mean NBRCS family and those with the lowest mean power levels, Galileo and BDS, form the second.

Given the fact that GMF based wind speed retrievals using NBRCS as inputs typically apply the same functional retrieval form to measurements arising from all transmitters, the results explored in this section highlight the fact that observed σ_0 biases may lead to GNSS system-specific offsets that are on the order 0.57 m/s on average for retrieved medium winds given a comparable set of NBRCS estimates and up to 5 m/s for high winds.

V. Noise Environment Dependencies

The estimation of noise power levels is also an integral step in the L1 calibration process. This is accomplished using portions of the DDM into which no received signal power maps (which then represents 'noise-only' power). An average or median of the power within this delay/Doppler space then provides an estimate of a measurement's noise floor, which then includes contributions both from noise internal to the receiver and external microwave radiation from the Earth's surface.

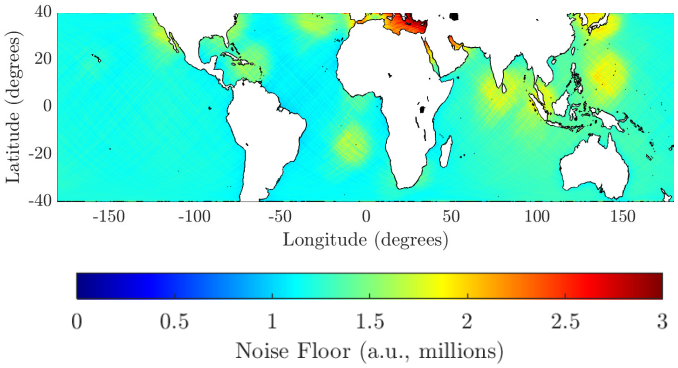

Fig. 4: Spire receivers' mean noise floor map projected on 0.25°×0.25° grid.

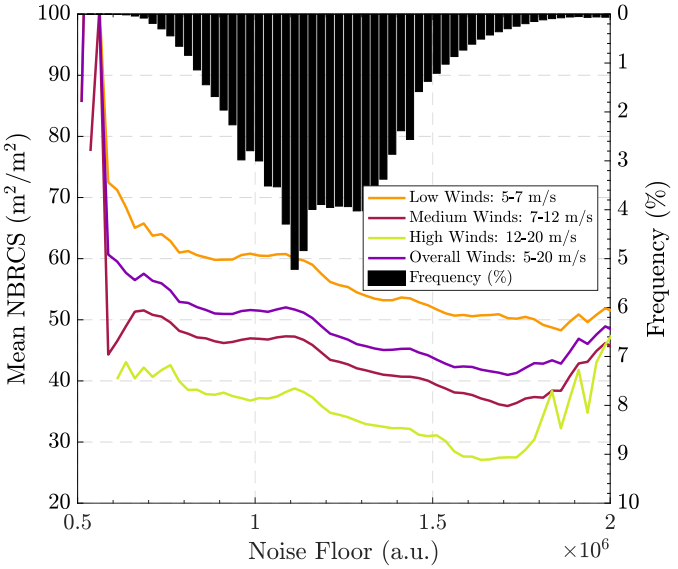

Fig. 5: Spire LEMUR-2 receivers' NBRCS mean μ as a function of noise floor estimates binned within low, medium and high wind speed regimes.

The dynamic external noise environment in which GNSS-R receivers operate also makes them susceptible to interference from ground based sources of interference and to nuisance signal reflections from other L-band GNSS systems. References [13], [14] in particular highlight the potential for GNSS Space Based Augmentation System (SBAS) transmissions to offset regional noise floor estimates and to induce an NBRCS/noise floor correlation for CYGNSS. Fig 4 reports a similar analysis for Spire measurements, and shows that noise floor estimates appear to be susceptible to similar effects in regions known to be conducive to higher rates of interference. In the Middle Eaast/North Africa region, a combination of GNSS signal 'jamming' and 'spoofing' activities increases the mean noise floor by ≈10 dB relative to the global average. Other 'hot spots' show a 2-5 dB noise floor increase due to interference related to the Wide Area Augmentation System (WAAS), GPS-aided GEO augmented navigation (GAGAN) and other SBAS systems.

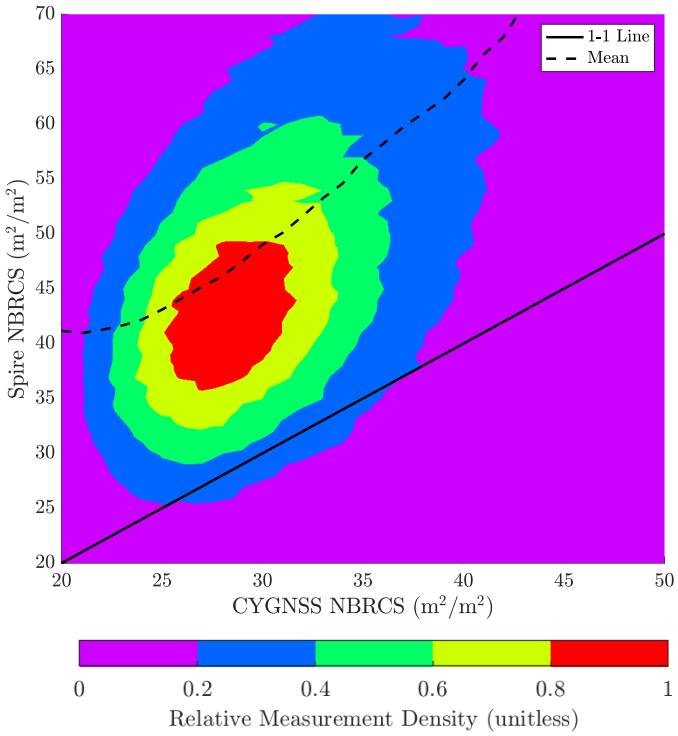

Fig. 6: Density plot summarizing co-located Spire/CYGNSS NBRCS observations occurring within 25 km footprints, separated by a maximum of 15 minutes and tracking the same PRN using ≈2.8 million measurements meeting these criteria.

Fig. 5 further plots mean NBRCS estimates versus the noise floor level, and shows a direct negative correlation across all wind speed regimes and incidence angles. These results indicate that Spire's σ_0 estimates undergo a sustained decrease as the noise floor estimate increases, which is expected to be especially impactful in the regions showing increase noise floor levels in Fig. 4. Given a comparable set of surface winds, the results depicted in Fig. 5 produce NBRCS variations of a 19.63 %, 33.16 %, and 18.86 % variability relative to the mean in the low, medium and high wind regimes respectively.

It is also noteworthy that patterns of increased noise floor powers often also coincide with regions where the receivers' S-band communication systems is activated, which suggests the potential of S-band communications link interference.

VI. Inter-constellation Comparisons

The availability of an extensive data record of ocean surface specular measurements provided by the CYGNSS constellation provides the opportunity to analyze the Spire observatories' overall correspondence to independent NBRCS estimates made over comparable surface conditions. Given the anticipated presence of various modest biases across both the CYGNSS and Spire constellations, this analysis is primarily intended to provide a qualitative assessment of the overall 'likeness' of both sets of measurements given their identical fundamental GNSS-R operation within the L-band.

The relevant measurements are defined as those occurring within a common 25 km footprint and separated by no more

than 15 minutes as to ensure that surface conditions have not undergone appreciable variability over most locations, so that observed NBRCS variability may reasonably be attributed to calibration variability. Additionally the pool of co-located measurements is limited to only those having SNRs greater than 3 dB (CYGNSS) and reflectivity greater than -10 dB (Spire) with the Spire and CYGNSS observatories tracking the same PRNs as to further exclude any measurement dependencies on PRN specific properties. In the comparisons depicted in Fig. 6 ≈2.8 million measurements are found to meet these criteria. The overall NBRCS behavior across both systems is found to be highly complementary across all reference surface conditions, with correlations estimated at the 79.03% level and unbiased Root Mean Square Difference (ubRMSD) on the order of 2.17 m^2/m^2. Residual calibration dependencies across both systems are also noted as evidenced by the ≈1.58 m^2/m^2 overall bias and ≈20 m^2/m^2 offset relative to the 1-1 line in Fig. 6. While the presence of bias is a general indicator of disparities in the systems' level of dependence on various calibration terms including antenna gain, receiver gain, hardware thermal dependencies, estimates of transmitted power, incidence angle, range terms and the like, the overall trends observed in Fig. 6 highlight the utility of the measurements provided by Spire's two batch 1 'LEMUR-2' for ocean surface wind sensing and related applications.

VII. Conclusion

This work provided an assessment of the Level-1 calibration quality of the two Spire batch-1 GNSS-R receivers over ocean surfaces. The results show a high degree of inter-channel interoperability of the related NBRCS estimates with overall biases limited to the 1% level on average. Apparent impacts of the observation geometry, transmitter properties, and external noise environment on the L1 calibration process were all observed and described.

A 3.91% mean NBRCS variability in excess of that predicted by model NBRCS estimates over a wide range of incidence angles was noted, with a ≈5 m^2/m^2 mean bias observed across various transmitter constellations. Interference due to S-band communications systems noise and external L-band interference was also shown to induce an NBRCS correlation to noise floor estimates such that NBRCS estimates were offset by 18.86%-33.16% depending on the level of noise estimates. Finally, a qualitative assessment of the overall NBRCS behavior relative to independent CYGNSS observations was presented highlighting correlations of approximately 79%, emphasizing the utility of FM109's and FM110's NBRCS estimates for ocean surface wind sensing.

References

[1] Y. Wang and Y. Morton, "Coherent GNSS Reflection Signal Processing for High-Precision and High-Resolution Spaceborne Applications," *IEEE Trans. Geosci. Remote Sens.*, pp. 1-12, 2020.

[2] A. Balakhder, M. Al-Khaldi and J. Johnson, "On the Coherency of Ocean and Land Surface Specular Scattering for GNSS-R and Signals of Opportunity Systems," *IEEE Trans. Geosci. Remote Sens.*, pp. 1-11, 2019.

[3] M. M. Al-Khaldi, J. T. Johnson, S. Gleason, E. Loria, A. J. O'Brien and Y. Yi, "An Algorithm for Detecting Coherence in Cyclone Global Navigation Satellite System Mission Level 1 Delay Doppler Maps," *IEEE Trans. Geosci. Remote Sens.*, 2020.

[4] D. Masters et al., "Status and Plans For Spire's Growing Commercial Constellation of GNSS Science Cubesats," *Joint 6th ROM SAF User Workshop and 7th IROWG*, Sep 2019, Konventum, Helsingør (Elsinore), Denmark.

[5] S. Gleason, "Algorithm Theoretical Basis Document (ATBD): Level 1A DDM Calibration Technical Memo," 2018.

[6] S. Gleason, "Algorithm Theoretical Basis Document (ATBD): Level 1B DDM Calibration Technical Memo," 2018.

[7] V. Zavorotny and A. Voronovich, "Scattering of GPS signals from the ocean with wind remote sensing application," *IEEE Trans. Geosci. Remote Sens.*, vol. 38, no. 2, pp. 951-964, 2000.

[8] T. Elfouhaily, B. Chapron, K. Katsaros and D. Vandemark, "A unified directional spectrum for long and short wind-driven waves," *Journal of Geophysical Research: Oceans*, vol. 102, no. 7, pp. 15781-15796, 1997.

[9] T. Wang, V. Zavorotny, J. Johnson, C. Ruf and Y. Yi, "Modeling of Sea State Conditions for Improvement of Cygnss L2 Wind Speed Retrievals," in *Proc. IEEE Int. Geosci. Remote Sens. Symp. (IGARSS)*, 2018.

[10] F. Said, Z. Jelenak, P. Chang and S. Soisuvarn, "An Assessment of CYGNSS Normalized Bistatic Radar Cross Section Calibration," *IEEE IEEE J. Sel. Topics Appl. Earth Observ. Remote Sens.,* vol. 12, no. 1, pp. 50-65, 2019.

[11] T. Wang, C. S. Ruf, B. Block, D. S. McKague, and S. Gleason, "Design and performance of a GPS constellation power monitor system for improved CYGNSS L1B calibration," IEEE IEEE J. Sel. Topics Appl. Earth Observ. Remote Sens., vol. 12, no. 1, pp. 26–36, Jan. 2019.

[12] P. Steigenberger, S. Thoelert and O. Montenbruck, "GNSS satellite transmit power and its impact on orbit determination," *Journal of Geodesy*, vol. 92, no. 6, pp. 609-624, 2017.

[13] S. Gleason, M. Al-Khaldi, C. Ruf, D. McKague, T. Wang and A. Russel, "Characterizing and Mitigating Digital Sampling Effects on the CYGNSS Level 1 Calibration," *IEEE Trans. Geosci. Remote Sens.*, vol. 60, pp. 1-12, 2022.

[14] S. Gleason, J. Johnson, C. Ruf and C. Bussy-Virat, "Characterizing Background Signals and Noise in Spaceborne GNSS Reflection Ocean Observations," *IEEE Geosci. Remote. Sens. Lett.*, vol. 17, no. 4, pp. 587-591, 2020.